Homo- to Co-Polyester Conversion in the Absence of Reagents Facilitated by a Dual Catalytic Process Involving Hydrogen Borrowing

Frederik Rummel,[a] Afiq Anuar,[b] Yu Qiang,[b] Matthias Rohmer,[a] Frerk-Ulfert Wehmeyer,[a] Matthias Vogt,[a] Frederik Haase,[a] Wolfgang Binder,[a] Kay Saalwächter,[b] Thomas Thurn-Albrecht,[b] Robert Langer[a,*]

[a]F. Rummel, M. Rohmer, F.-U. Wehmeyer, Dr. M. Vogt, JunProf. Dr. F. Haase, Prof. D. W. Binder, Prof. Dr. R. Langer
Institute of Chemistry, Faculty of Natural Sciences II, Martin-Luther-University Halle-Wittenberg, 06120 Halle, Germany
E-mail: robert.langer@chemie.uni-halle.de

[b]A. Anuar, Y. Qiang, Prof. Dr. K. Saalwächter, Prof. Dr. T. Thurn-Albrecht, Institute of Physics, Faculty of Natural Sciences II, Martin-Luther-University Halle-Wittenberg, 06120 Halle, Germany

KEYWORDS Metal-Ligand-Cooperation • Hydrogen Borrowing • Homogeneous Catalysis • Pincer Ligand • Polymer Reaction

ABSTRACT: A ruthenium-catalyzed hydrogen transfer ester metathesis (HTEM) is reported that allows for the isomerization of a linear polyester such as polycaprolactone (PCL) without the need for any stoichiometric reagent, forming a novel type of co-polyester containing additional hexylene adipate (HA) repeating units. Mechanistic investigations show that the formation of the chemically modified polyester relies on a two-fold catalytic reaction; a HTEM via a hydrogen borrowing process and a concomitant transesterification catalyzed by the base co-catalyst. Evidence is provided that the hydrogen transfer ester metathesis proceeds via a reversible aldehyde formation. The described HTEM represents an unprecedented catalyzed hydrogen borrowing process within polymers – and bears significant importance regarding a dynamic post-synthetic modification of polyesters.

INTRODUCTION

Metal-Ligand-Cooperativity has been a key concept for the development of homogeneous catalyst for novel atom economic and sustainable reactions with molecular substrates in the last two decades. Recent advancements of such metal-ligand-cooperative catalysis particularly involve hydrogenation, dehydrogenation and dehydrogenative coupling reactions as well as hydrogen borrowing-type reactions.[1,2,11–13,3–10] These important developments were also applied for the synthesis of polyesters[14–16] and -amides[17–20] by dehydrogenative coupling, as well as for alternative strategies for the recycling of polyester,[21–24] -amides[25,26] and -urethanes[26] by hydrogenation (Fig. 1 **A**), but the huge number of catalytic hydrogen borrowing type protocols in organic synthesis have never been applied to polymers (Fig. 1 **B**),[27] although this can potentially provide access to new types of polymeric materials and can be also used to tune the chemo-physical properties of the material.

Polyesters are of increasing importance as they can function as substitutes for other bulk – and commodity polymers, due to their high potential with respect to chemical recycling and biodegradability, but methodologies to achieve their recycling, degradation and valorization, as well as the optimization of their properties, still require significant improvement. Important milestones have been the introduction of covalent adaptive networks (CANs) and so-called vitrimers, which rely on a catalytic transesterification reaction at elevated temperature,[28,29] as well as the discovery that aliphatic long-chain polyester, which can be produced from renewable feedstocks and recycled by transesterification, exhibit properties similar to high-density polyethylene (HDPE).[30,31] In this context, the modification of polymers exhibits a great potential

and can produce unusual properties, such as enormous electro-[32] and barocaloric effects,[33] but methods for the post synthetic modification of polyesters, yielding functionalized polymers with tuned properties, are often limited to blending, curing, grafting or derivatization with reagents,[32–39] whereas the modification of the main chain or back bone often involves specifically designed polymers.[40,41] In particular for statistic co-polyesters, formed by random incorporation of a second minor monomer in polyesters, it has been demonstrated that biodegradation can be facilitated, while important properties of the original polyester are maintained.[42]

In the current manuscript, we report a novel type of transesterification reaction for polyesters that relies on a hydrogen transfer ester metathesis (HTEM) sequence (Fig. 1 **C**), which represents the first example of a catalytic hydrogen borrowing reaction with polymers as substrates. The combination of the latter with a concurrent catalytic transesterification allows for a dual catalytic system, which gives rise to the efficient main chain modification and conversion of a homo-polyester into block - or randomly sequenced co-polyester in the presence of a suitable cooperative catalyst-system and in the absence of any reagent. It is demonstrated that with formation of constitutional isomers, the properties of the utilized polyester can be modified in an atom-economic reaction.

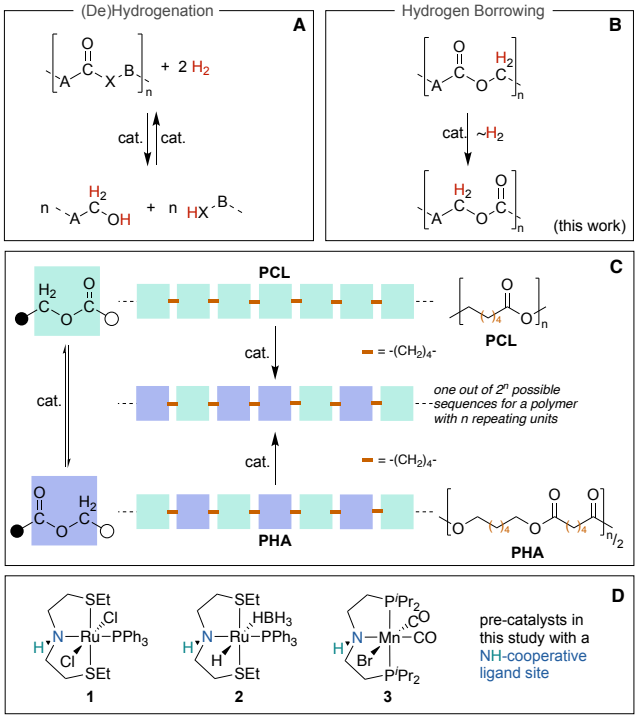

Figure 1. Previously reported dehydrogenative polymer synthesis and hydrogenative depolymerization (**A**) and the novel introduced hydrogen borrowing reaction in this work (**B**). Concept of the hydrogen transfer ester metathesis of polyesters using the example of polycaprolactone (**C**) as well as potential pre-catalysts (**D**).

RESULTS AND DISCUSSION

Aliphatic linear polyesters of different chain lengths, such as semi-crystalline polycaprolactone (PCL), are ideal model substrates to transfer the reactivity from molecular esters[43] to polyesters, as their morphology and the role of entanglements is well understood. Using the previously optimized conditions for molecular esters, we utilized 1 mol% of complex **1** with respect to the average number of ester groups (M) together with 5 mol% of KO^{t}Bu co-catalyst (B) in the reaction of PCL (M_n = 5 - 54 kDa) in toluene-d_8 at different temperatures. We analyzed the resulting reaction mixture by gel permeation chromatography (GPC), as well as NMR spectroscopy (Table 1).

The reaction of PCL (M_n = 5 kDa) at 80 °C yields a polyester with reduced molecular weight of M_n = 3 kDa (Entry 1) after 16 h. The ^{1}H NMR spectrum of the reaction did not show any diagnostic changes, due to superimposed resonances. However, by comparison of the ^{13}C{^{1}H} NMR spectra of reference samples, including PCL + KO^{t}Bu, polyhexylene adipate (PHA) and PHA + KO^{t}Bu, we identified hexylene adipate (HA) as major new monomer in the formed polyester with a characteristic chemical shift of 173.42 ppm for the carbonyl carbon atom, which is the exact value, reported for HA segments in block copolymers.[44] As the resonances of the -*C*H$_2$COO-protons in CL- and HA-units exhibit similar relaxation times in the ^{13}C{^{1}H} NMR spectrum (Fig. S11/S12), we used the integrals of these resonances to estimate the overall fraction of CL and HA monomers in the formed copolymers and monitor the progress of the reaction. This analysis revealed that the low molecular weight PCL (M_n = 5 kDa) contains 67 % CL monomer units and 33 % HA monomer units

after the catalytic reaction (16 h) in the presence of 1 mol% of **1** and 5 mol% KO^{t}Bu (Entry 1, two CL units are converted to one PHA unit and are weighted accordingly). The catalyst system in this mixture remains active and continuous heating for overall 122h yields a co-polyester with 56 % CL and 44 % HA monomers. To evaluate the influence of the base we synthesized the new hydrido borohydrido pre-catalyst **2** (Fig. 1 **B**). This complex is isolable and was fully characterized.[45] Catalyst **2** does not require the presence of a base co-catalyst for pre-catalyst activation. Interestingly, complex **2** as pre-catalyst in the absence of KO^{t}Bu as co-catalyst, exhibits significantly reduced activity and yields only 9 % of HA under otherwise identical conditions after 16 h (Entry 2). High molecular weight PCL (M_n = 54 kDa) displays a similar reactivity with 1 mol% complex **1** and 5 mol% KO^{t}Bu, yielding 30 % of HA monomers after 16 h at 80 °C, but with significantly reduced molecular weights (M_n = 4 kDa, Entry 3). Again, continuous heating yields a similar HA fraction of 44 % after 130 h like with the low molecular weight PCL. The utilization of 0.5 mol% of complex **1** in combination with 2.5 mol% of KO^{t}Bu results in the formation of 21 % HA at 80 °C after 16 h (Entry 4). The catalytic HTEM of PCL takes place at ambient temperature as well (Entry 5). With complex **1** and KO^{t}Bu as co-catalyst the reaction is significantly slower after 4 h at ambient temperature, but shows the same conversions after 16 h and finally yields a similar fraction of 43 % HA after 130 h, suggesting that catalyst deactivation is more facile at elevated temperatures. Overall, for different molecular weight and different reaction conditions the formation of 43 to 45 % of HA seems to be thermodynamically favorable (Figure 2), indicating that there is a thermodynamic minimum P(CL-HA)-composition, which is different from 50%.

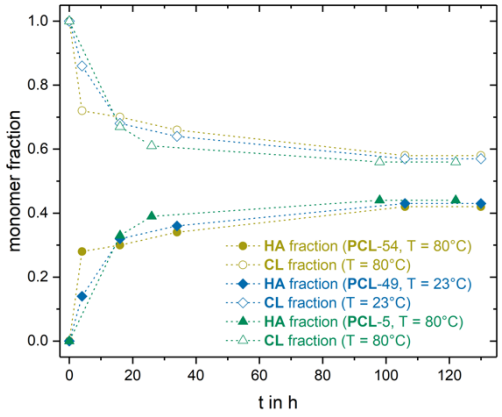

Figure 2. Conversion of CL- to HA-units for different starting materials and reaction conditions .

The utilization of **2** for the HTEM of high molecular weight PCL in the absence of KO^{t}Bu results in the formation of smaller amounts of HA at 80 °C (Entry 6), indicating that KO^{t}Bu is crucial to achieve high activity in this reaction. For this reason, control experiments were performed, in which PCL was heated in the absence (Entry 7) and in the presence of 5 mol% KO^{t}Bu (Entry 8) for 16 h in toluene. In the absence of base, no conversion and no significant change in the molecular weight distribution is observed, whereas the presence of KO^{t}Bu reduced the average molecular weight from M_n = 54 kDa to M_n = 10 kDa. Notably, the employment of a non-nucleophilic base like 1,8-diazabicyclo[5.4.0]undec-7-en (DBU) did not result in any conversion and the $^{31}P\{^1H\}$ NMR spectrum of the reaction mixture confirmed that activation of pre-catalyst **1** does not take place with DBU. To verify the hypothesis of a thermodynamic minimum with a well-defined HA content, we utilized PHA with a different molecular weight of M_n = 8 kDa. With 1 mol% of complex **1** as pre-catalyst and 5 mol% KO^{t}Bu co-catalyst, however, only a small conversion of PHA is observed after 16 h, but further addition of complex **1** (1 mol%) along with additional 5 mol% of KO^{t}Bu resulted in the formation of an almost identical HA content of 45 % after 32 h (Entry 9). These findings indicate that the reaction with PHA is significantly slower than with PCL, however strongly suggesting the presence of a thermodynamically favored constitution of approx. 45 % HA and 55 % CL. Recently, manganese pincer-type complexes have been demonstrated to exhibit comparable or even better catalytic activities in reactions involving dihydrogen than corresponding ruthenium complexes.[46,47,56–62,48–55] For this reason, we tested [(^{i}Pr-PN^{H}P)MnBr(CO)$_2$][63–69] (**3**) as a potentially more sustainable pre-catalyst under optimized conditions (Entry 10). To our surprise no formation of HA units was observed by NMR spectroscopy, although ^1H and $^{31}P\{^1H\}$ NMR spectra clearly indicated activation of **3**.

Table 1. Catalytic conversion of different polyesters using hydrogen transfer ester metathesis.

Entry [b]	polymer	M_n/M_w[a] [kDa]	PD[a]	C	M/B/C[b]	T [°C]	t [h]	%PCL[c]	%PHA[c]	M_n/M_w[a] [kDa]	PD[a]	TON
1	PCL	5 / 6	1.22	1	100/5/1	80	16	67	33	3 / 4	1.47	33
2	PCL	5 / 6	1.22	2	100/0/1	80	168	91	9	3 / 6	1.98	9
3	PCL	54 / 93	1.72	1	100/5/1	80	16	70	30	4 / 7	1.65	30
4	PCL	54 / 93	1.72	1	200/5/1	80	16	79	21	9 / 15	1.77	42
5	PCL	54 / 93	1.72	1	100/5/1	23	16	68	32	7 / 17	2.53	32
6	PCL	49 / 83	1.69	2	100/5/1	80	168	85	15	4 / 15	4.29	15
7	PCL	54 / 93	1.72		100/0/0	80	16	100	0	52 / 96	1.83	0
8	PCL	54 / 93	1.72		100/5/0	80	16	100	0	10 / 23	2.84	0
9	PHA	8 / 13	1.54	1	50/5/1	80	32	55	45	4 / 5	1.44	27
10	PCL	49 / 83	1.69	3	100/5/1	80	16	100	0	-	-	0

a) based on GPC in THF. B) the utilized number of ester groups (M) to base (B) and pre-catalyst (C) ratios based on M_n. c) obtained by integration of selected resonances in the $^{13}C\{^1H\}$ NMR spectra, for which the relaxation times are determined by inversion recovery experiments to be similar. This approach was further validated by ^{13}C NMR measurements with different relaxation delays, which gave almost identical integral ratios.

As the change in molecular weight of the starting material PCL and the obtained polyester was the smallest for the low molecular weight PCL (M_n = 5 kDa), we focused on analyzing the exact identity of these samples. Mass spectrometric investigations using matrix-assisted laser desorption ionization (MALDI) confirmed the findings observed by NMR spectroscopy and GPC. As the molecular mass of a HA units is the same as two CL units and both, tandem mass spectrometry experiments were performed using MALDI TOF-TOF MS to investigate the composition after the catalytic reaction. By comparison of the fragmentation mass spectrum (Fig. S2) of the PCL starting material and the formed P(CL-HA)-copolymer for selected mass peaks (e.g. 1513 m/z) several additional ion peaks were identified in the P(CL-HA)-copolymer (e.g. $[C_6H_8O_3+H]^+$ at 129 m/z or $[C_{12}H_{18}O_4+H]^+$ at 227 m/z), which clearly indicate the presence of adipic acid ester units together with CL units.

In line with the reduced molecular weight and the changed polymer distribution of PCL after the catalytic reaction a lower melting temperature (T_m) is observed by differential scanning calorimetry (DSC) in the 2nd heating run with respect to the starting material (Fig. 3 and Table 2). The melting curve of PCL is basically reproduced after the catalytic reaction but with broader curves, indicating a wider melting temperature range. Isodimorphic co-crystallisation is often observed for related statistical co-polyesters,[42,70] but with PCL as starting polyester an additional crystallisation peak (T_c) is observed from the 1st cooling run after hydrogen transfer catalysis with respect to the unmodified PCL. This is in contrasts to an isodimorphic semi-crystalline structure, resulting from co-crystallisation, and rather suggests phase separation of a second component. The chemical modification of ester groups in polycaprolactone (PCL) in line with the formation of HA units is expected to have a general impact on chemical properties such as the crystallisation behaviour or -kinetics. Such a thermal behaviour of the formed co-polyester is usually not observed for PCL samples and might be an indication of ester-layer disorder of the crystalline stems.[71]

Table 2. Differential scanning calorimetry parameters for PCL before and after the catalytic hydrogen transfer ester metathesis.

PCL	M_n/M_w [kDa]	PD	T_m / °C	T_c / °C
before HTEM	5 / 6	1.22	43.4 / 47.7	25.1
after HTEM	3 / 4	1.47	34.8 / 40.6	14.5 / 5.4

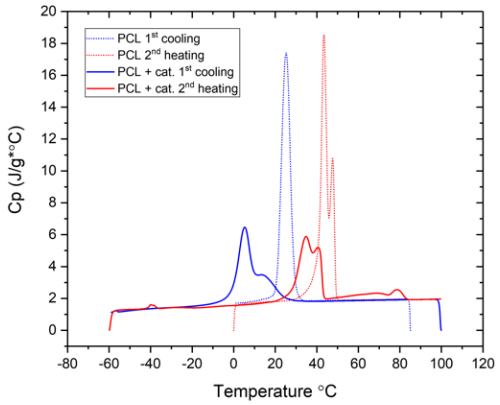

Figure 3. Differential Scanning Calorimetry (DSC) diagram of the PCL (M_n = 5 kDa starting material) sample before and after the catalytic reaction.

^{1}H static and ^{13}C MAS solid-state NMR spectroscopy were used to further investigate the impact of the hydrogen transfer ester metathesis (HTEM) in PCL. Samples of PCL before and after the catalytic reaction in toluene were carefully dried in vacuo and isothermally crystallized at 30 °C (27 °C) for 24 h, prior to solid-state NMR measurements. ^{1}H FID NMR measurements enable a direct estimation of the mass crystallinity by 3-component fitting (adding an amorphous yet immobilized interphase), based on the dependence of the ^{1}H transverse (T_2) relaxation behaviour on molecular mobility (the crystalline phase has a short-T_2 Gaussian decay reflecting its rigidity). They show that the crystalline fraction in both cases is decreasing with increasing temperature, whereas the product from HTEM results in an overall decrease of the crystalline fraction by only 10-15 % (e.g. from 60.3 to 45.1 at 20 °C) with concomitant increase of an amorphous fraction, but with a decrease of the interphase fractions. In addition to the overall increase of the amorphous fraction, the decreasing interphase fraction indicates the presence of thicker amorphous and crystalline domains after the catalytic reaction.

As crystalline segments in the polymer give rise to long ^{13}C spin-lattice relaxation times ($T_{1,C} > 10$ s) in solid-state NMR spectra (^{13}C MAS NMR), and amorphous segments are rather characterized by short ^{13}C spin-lattice relaxation times, ^{13}C MAS NMR spectroscopy with spin–lattice relaxation filtering can be used to detect and distinguish resonances of the crystalline, intermediate, and highly mobile amorphous phases of the utilized PCL before and after the catalytic reaction. This approach is non-quantitative, but enables the identification of certain chemical motifs present in the different phases. The ^{13}C cross polarization MAS NMR spectrum with 2 ms contact time of the PCL after the catalytic reaction displays additional resonances and shoulders with respect to the untreated PCL, which arise from ester groups of amorphous, crystalline and interphase regions. In particular, the resonances assigned to the carbonyl carbon atoms of the polyester are diagnostic for the progress of the investigated HTEM reaction. In line with the observations by solution NMR, a resonance at 174.7 ppm of medium intensity is observed in addition to the original resonance of the homo-polymer at 173.8 ppm with a shoulder at 173.2 ppm (Fig. 4). In addition, a new resonance of comparably low intensity is observed at 181.1 ppm.

The ^{13}C CP MAS NMR spectrum with a short contact time of 0.2 ms displays mostly resonances of crystalline segments, which in case of the investigated PCL results in the appearance of two resonances in the carbonyl region. The resonance at 173.8 ppm is observed in the starting material as well, whereas the additional resonance at 174.7 ppm was newly observed after the catalytic reaction. Notably, we conclude that the newly formed HA units become part of the (co)crystal.

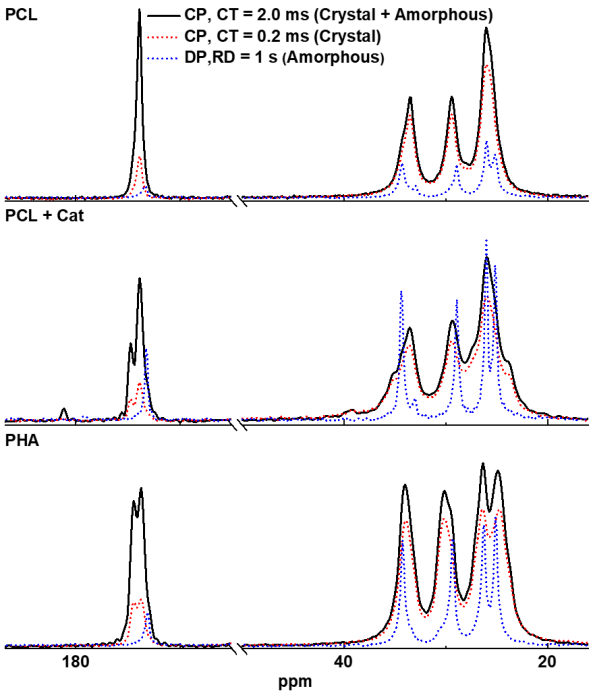

Figure 4. Diagnostic regions of MAS ^{13}C NMR spectra of PCL, PHA and PCL after hydrogen transfer ester metathesis, showing resonances of amorphous segments (blue), crystalline segments (red) and the combination of both (black).

Direct polarization (DP) excitation with a short recycle delay of 1 s was used to detect resonances of the highly mobile, amorphous components in the ^{13}C MAS NMR spectrum, which displays only one resonance at 173.2 ppm that appeared as a shoulder in the ^{13}C CP NMR spectrum with 2 ms contact time. Assuming that the small resonances close to the major carbonyl resonance at 172.21 ppm in the solution ^{13}C NMR spectrum are not resolved in the solid-state ^{13}C NMR spectra, we assigned the new additional resonance at 174.7 ppm after catalysis to the newly formed HA units, which are thus found to represents the second major species in crystalline segments.

Wide-angle X-Ray diffraction (WAXD) of isothermally crystallized samples was performed to receive further insights on the composition of the crystalline phase (Fig. 5). Characteristic peaks were observed at angles $2\theta = 21.4°$ and 23.8° for the PCL starting material, which were assigned to the (110) and (200) planes, respectively.[72] However, crystalline PHA gives rise to very similar characteristic reflexes at 21.3° and 23.9°, which were assigned to the 220 and 040 plane.[73] In addition to the similar diffraction patterns of PCL and PHA, it has been demonstrated that blends of both polymers do not give rise to new reflections,[74] indicating the absence of new crystalline domains. The disappearance of the reflections at the higher temperature (110 °C) is in line with the melting temperature observed in DSC.

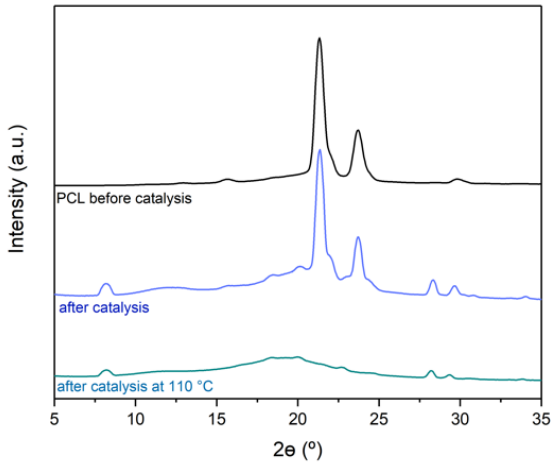

Figure 5. Wide-angle X-Ray diffractogram of PCL before (top) and after the catalytic reaction (middle) at ambient temperature, as well as at 110 °C, above the melting temperature of PCL.

Further evidence for the identity of the modified PCL is provided by IR spectroscopy (Fig. 6). In agreement with the frequency analysis of dimers, trimers and tetramers by quantum chemical methods, the bands associated with the C=O stretching vibration of the ester groups in the IR spectrum of the dried samples are not indicative for the analysis of the reaction and showed only a small shift of a comparably broad band from 1720 to 1722 cm^{-1}. However, previous reports identified bands in the IR spectra, which are unique for crystalline PHA[74,75] and for PCL.[74] The IR spectrum of PCL after the catalytic reaction shows bands that are unique to crystalline PHA. The observation of these bands may be explained by the formation of larger PHA sequences or just HA inclusion in the crystalline domains in addition to sequences detected by tandem mass spectrometry.

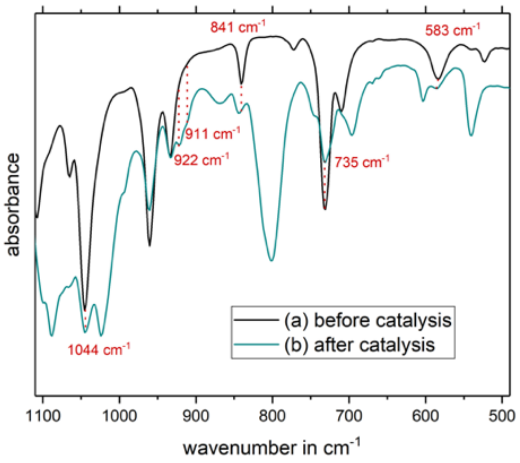

Figure 6. Diagnostic region of the IR spectrum of PCL before and after hydrogen transfer ester metathesis (HTEM).

As the ester groups in PCL, PHA and the polyesters formed by HTEM are very similar, it can be assumed that the main driving force for the observed catalytic reaction is entropy and possibly the preferential stability of certain PHA-PCL sequences. To gain further insights on the possible driving force for the reported HTEM, we performed quantum chemical investigations of small oligomers with three to five lactone repeating units to identify potentially more stable sequences. Following a protocol that involves conformational pre-optimization using the materials studio program package, we performed density functional theory (DFT) calculations of the pre-optimized structures on B97D3/def2-TZVP level of theory with a solvent correction, using the Polarizable Continuum Model (PCM) for toluene, for all 2^n possible constitutional isomers that can be formed by the hydrogen transfer ester metathesis, where n is the number of linking ester groups (n = 2 - 4). It turns out that the calculated difference in Gibbs energy of certain sequences with respect to PCL varies over a range of -11 to + 33 kJ/mol, indicating that a number of sequences are of comparable stability as the sequence in PCL, whereas the formation of several sequences seems thermodynamically less favorable. As the catalytic reactions with PCL and PHA result in almost identical PCL/PHA ratios after long reaction times, the existence of a thermodynamically favorable composition is likely, although the difference in Gibbs energy might be small. As hydrogen liberation needs to be avoided for the reaction to proceed, the HTEM has to be conducted in closed vessels, which in case of polyesters means that the utilized catalysts (**1** and **2**) will simply equilibrate the PCL or PHA on a quite flat potential energy surface.

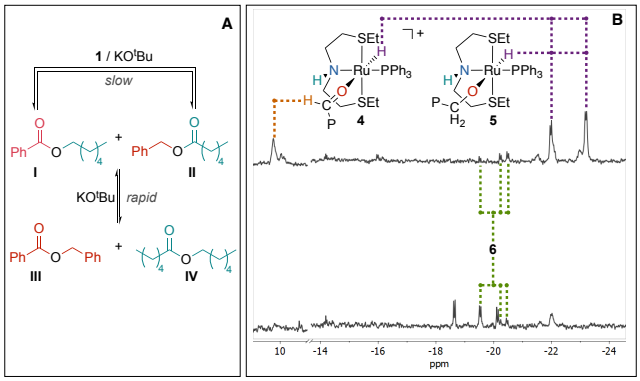

Figure 7. Observed catalytic reactions for molecular esters (**A**). Selected regions of the 1H NMR spectra of the catalytic reaction with PCL after 16 h reaction at 80 °C in toluene-d_8 under optimized conditions (top) and with reduced pressure for the last hour of the reaction (bottom) (**B**).

As the KO^{t}Bu co-catalyst seems to have a crucial role for the observed catalytic activity, we investigated the underlying catalytic reaction with molecular ester in more detail. Applying optimized reaction conditions (toluene, 80 °C, 16h, closed vessel) the reaction with hexyl benzoate (**I**) is in principle expected to result in the formation of four esters (**I-IV**, Fig. 7 A). Benzyl hexanoate (**II**) is directly formed by HTEM, whereas the esters **III** and **IV** are formed by a regular transesterification of a mixture of **I** and **II**. It is demonstrated that neither complex **1** in the absence of KO^{t}Bu nor pure KO^{t}Bu are catalytically active in the hydrogen transfer ester metathesis reaction. As bases such as KO^{t}Bu are known to catalyze transesterification reactions without hydrogen transfer,[76] a mixture of the symmetric esters **III** and **IV** was used as substrate to investigate the influence of base catalyzed transesterification in the investigated reaction. It turns out, that in the presence of **1**/KO^{t}Bu the formation of equimolar amounts of **I-IV** is observed at ambient temperature in less than one hour. An identical observation is made with KO^{t}Bu as catalyst, suggesting that with the utilized combination of pre-catalyst and base co-catalyst two catalytic reactions are involved: a comparably slow HTEM and a rapid, base catalyzed transesterification. With respect to the reported polyester reaction the KO^{t}Bu catalyzes a rapid regular transesterification of polyester chains, which might be responsible for the formation sequences of blocks after the actual hydrogen transfer step(s).

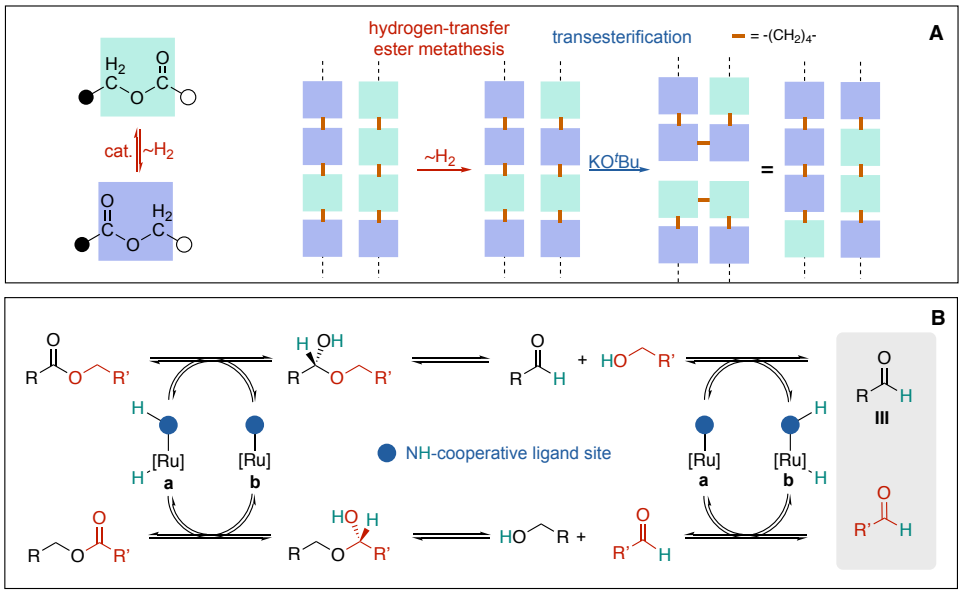

Figure 8. Illustration of hydrogen transfer ester metathesis with subsequent transesterification (A) as well as the anticipated, simplified mechanism for the hydrogen transfer ester metathesis (**B**).

Pre-catalyst **1** is known for its high catalytic activity in the hydrogenation of esters and the acceptorless dehydrogenation of primary alcohols. For these reactions, the two active species *fac*-[(SNS)Ru(H)$_2$(PPh$_3$)] and *mer*-[(SNS)Ru(H)(OEt)(PPh$_3$)]·EtOH that are involved in the catalytic cycle could be isolated and partially characterized (SNS = {EtSCH$_2$CH$_2$}NH).[77] As the reported HTEM is conducted in a close system, whereas acceptorless dehydrogenations are typically conducted in an open system or a stream of inert gas and hydrogenations under hydrogen pressure, ^{1}H and ^{31}P{^{1}H} NMR spectra of the reaction mixture were acquired to identify decomposition products as well as potential resting states or active species (Fig. 7 **B**). The ^{1}H NMR spectra of the reaction mixtures with PCL of different lengths in toluene-d_8 after 16 h displays two doublet resonances of similar intensity at -21.97 ppm ($^2J_{PH}$ = 23.5 Hz) and -23.19 ppm ($^2J_{PH}$ = 25.6 Hz) as well as three small resonances for the diastereomers of *mer*-[(SNS)Ru(H)Cl(PPh$_3$)]·(**6**).[78] In addition, a broadened resonance at 10.23 ppm with an integral associated with one proton with respect to one of the hydride resonances indicates the presence of an aldehyde or a coordinated aldehyde. The utilized SNS-ligand usually gives rise to different diastereomers in meridional coordination mode, differing in the orientation of the thioether groups.[77,78] The observed hydride species may therefore either originate from two diastereomeric hydrido aldehyde complexes or from two species with similar chemical environment (Fig. 7 **B**), such as a hydrido aldehyde complex (**4**) and a hydrido alkoxide complex (**5**). Notably, when the reaction conditions after 15 h at 80 °C of the HTEM are changed to a closed system with reduced pressure, which are conditions that typically favor acceptorless dehydrogenation, the resonance corresponding to an aldehyde disappeared and three new hydride isomers are formed. These findings provide further support for our hypothesis that the ester groups are partially reduced to aldehydes, which are reconnected by the catalyst.

Overall, these findings indicate that two catalytic reactions are involved in the formation of the novel type of polyesters reported herein (Fig. 8 A): (i) the ruthenium-catalyzed hydrogen transfer ester metathesis that results in chemically modified ester groups, and (ii) the base-catalyzed transesterification that facilitates a rapid chain exchange and equilibrates the system towards the most stable sequence(s). Both reaction involve an initial cleavage of an ester group and lead in case of (i) to a cleaved (aldehyde) resting state, which results in overall reduced molecular weights.

Based on our mechanistic investigations, as well as the previously reported mechanistic work for molecular systems,[79–83] a possible mechanism involves a number of hydrogenation and dehydrogenation steps resulting in a temporary cleavage of the ester group linkage via hemiacetal formation and its subsequent dissociation (Fig. 8 **B**). Dehydrogenation of the resulting alcohol group followed by hydrogenation of the initial aldehyde yields a new hemi-acetal, whose dehydrogenation finalizes the HTEM sequence.

CONCLUSION

In conclusion, we reported a catalytic reaction that allows to transfer a linear polyester such as polycaprolactone (PCL) into a novel co-polyester, consisting of an additional repeating unit without the need for any reagent. For different polyesters as starting materials, *i.e.* pure PCL and PHA, the reaction was found to yield polyesters of almost identical HA/CL ratios (45/55) after long reaction times, indicating the presence of a thermodynamic minimum ratio between the two polyesters. Our mechanistic investigations show that two catalytic reactions are operative under the employed conditions, a hydrogen transfer ester metathesis, resulting in truly chemically modified ester groups via hydrogen transfer reaction, and a (common) base-catalyzed transesterification. We further provide evidence that the hydrogen transfer ester metathesis (HTEM) proceeds via a reversible aldehyde formation. Notably, the crystallinity of the modified materials is only slightly reduced which suggests that mechanically attractive materials are formed. Of course, the reported polyester modification and the correspondingly reduced crystallinity are expected to have a significant impact on the physical and mechanical properties of the polyesters. Therefore, we are currently focusing our efforts on the application of the reported post-synthetic modification to tune properties and facilitate chemical recycling.

REFERENCES

(1) Khusnutdinova, J. R.; Milstein, D. Metal-Ligand Cooperation. *Angew. Chem. Int. Ed.* **2015**, *54* (42), 12236–12273. https://doi.org/10.1002/anie.201503873.

(2) Gunanathan, C.; Milstein, D. Applications of Acceptorless Dehydrogenation and Related Transformations in Chemical Synthesis. *Science (80-.).* **2013**, *341* (6143), 1229712–1229712. https://doi.org/10.1126/science.1229712.

(3) Gunanathan, C.; Milstein, D. Metal-Ligand Cooperation by Aromatization-Dearomatization: A New Paradigm in Bond Activation and “Green” Catalysis. *Acc. Chem. Res.* **2011**, *44* (8), 588–602. https://doi.org/10.1021/ar2000265.

(4) Kumar, A.; Gao, C. Homogeneous (De)Hydrogenative Catalysis for Circular Chemistry – Using Waste as a Resource. *ChemCatChem* **2021**, *13* (4), 1105–1134. https://doi.org/10.1002/cctc.202001404.

(5) Werkmeister, S.; Neumann, J.; et al. Pincer-Type Complexes for Catalytic (De)Hydrogenation and Transfer (De)Hydrogenation Reactions: Recent Progress. *Chem. - A Eur. J.* **2015**, *21* (35), 12226–12250. https://doi.org/10.1002/chem.201500937.

(6) Dub, P. A.; Ikariya, T. Catalytic Reductive Transformations of Carboxylic and Carbonic Acid Derivatives Using Molecular Hydrogen. *ACS Catal.* **2012**, *2* (8), 1718–1741. https://doi.org/10.1021/cs300341g.

(7) Schlagbauer, M.; Kallmeier, F.; et al. Manganese-Catalyzed β-Methylation of Alcohols by Methanol. *Angew. Chem. Int. Ed.* **2020**, *59* (4), 1485–1490. https://doi.org/10.1002/anie.201912055.
(8) Kallmeier, F.; Fertig, R.; et al. Chromium-Catalyzed Alkylation of Amines by Alcohols. *Angew. Chem. Int. Ed.* **2020**, *59* (29), 11789–11793. https://doi.org/10.1002/anie.202001704.
(9) Irrgang, T.; Kempe, R. 3d-Metal Catalyzed N- and C-Alkylation Reactions via Borrowing Hydrogen or Hydrogen Autotransfer. *Chem. Rev.* **2019**, *119* (4), 2524–2549. https://doi.org/10.1021/acs.chemrev.8b00306.
(10) Irrgang, T.; Kempe, R. Transition-Metal-Catalyzed Reductive Amination Employing Hydrogen. *Chem. Rev.* **2020**, *120* (17), 9583–9674. https://doi.org/10.1021/acs.chemrev.0c00248.
(11) Fertig, R.; Leowsky-Künstler, F.; et al. Rational Design of N-Heterocyclic Compound Classes via Regenerative Cyclization of Diamines. *Nat. Commun.* **2023**, *14* (1), 595. https://doi.org/10.1038/s41467-023-36220-w.
(12) Gorgas, N.; Kirchner, K. Isoelectronic Manganese and Iron Hydrogenation/Dehydrogenation Catalysts: Similarities and Divergences. *Acc. Chem. Res.* **2018**, *51* (6), 1558–1569. https://doi.org/10.1021/acs.accounts.8b00149.
(13) Subaramanian, M.; Sivakumar, G.; et al. Selective Hydrogenation of Primary Amides and Cyclic Di-Peptides under Ru-Catalysis. *Chem. Commun.* **2020**, *56* (82), 12411–12414. https://doi.org/10.1039/D0CC04550K.
(14) Manar, K. K.; Cheng, J.; et al. Promising Catalytic Application by Pincer Metal Complexes: Recent Advances in Hydrogenation of Carbon-Based Molecules. *ChemCatChem* **2023**, *15* (15). https://doi.org/10.1002/cctc.202300004.
(15) Hunsicker, D. M.; Dauphinais, B. C.; et al. Synthesis of High Molecular Weight Polyesters via in Vacuo Dehydrogenation Polymerization of Diols. *Macromol. Rapid Commun.* **2012**, *33* (3), 232–236. https://doi.org/10.1002/marc.201100653.
(16) Xu, W.-M.; Yu, Y.-D.; et al. Green Synthesis of Chemically Recyclable Polyesters via Dehydrogenative Copolymerization of Diols. *Chinese J. Polym. Sci.* **2023**. https://doi.org/10.1007/s10118-023-2903-9.
(17) Zeng, H.; Guan, Z. Direct Synthesis of Polyamides via Catalytic Dehydrogenation of Diols and Diamines. *J. Am. Chem. Soc.* **2011**, *133* (5), 1159–1161. https://doi.org/10.1021/ja106958s.
(18) Owen, A. E.; Preiss, A.; et al. Manganese-Catalyzed Dehydrogenative Synthesis of Urea Derivatives and Polyureas. *ACS Catal.* **2022**, 6923–6933. https://doi.org/10.1021/acscatal.2c00850.
(19) Brodie, C. N.; Owen, A. E.; et al. Synthesis of Polyethyleneimines from the Manganese-Catalysed Coupling of Ethylene Glycol and Ethylenediamine. *Angew. Chem. Int. Ed.* **2023**, *202306655*. https://doi.org/10.1002/anie.202306655.
(20) Kumar, A.; Armstrong, D.; et al. Direct Synthesis of Polyureas from the Dehydrogenative Coupling of Diamines and Methanol. *Chem. Commun.* **2021**, *57* (50), 6153–6156. https://doi.org/10.1039/d1cc01121a.
(21) Krall, E. M.; Klein, T. W.; et al. Controlled Hydrogenative Depolymerization of Polyesters and Polycarbonates Catalyzed by Ruthenium(II) PNN Pincer Complexes. *Chem. Commun.* **2014**, *50* (38), 4884–4887. https://doi.org/10.1039/c4cc00541d.
(22) Fuentes, J. A.; Smith, S. M.; et al. On the Functional Group Tolerance of Ester Hydrogenation and Polyester Depolymerisation Catalysed by Ruthenium Complexes of Tridentate Aminophosphine Ligands. *Chem. – A Eur. J.* **2015**, *21* (30), 10851–10860. https://doi.org/10.1002/chem.201500907.
(23) Westhues, S.; Idel, J.; et al. Molecular Catalyst Systems as Key Enablers for Tailored Polyesters and Polycarbonate Recycling Concepts. *Sci. Adv.* **2018**, *4* (8), 1–9. https://doi.org/10.1126/sciadv.aat9669.
(24) Knight, K. D.; Fieser, M. E. Divergent Methods for Polyester and Polycarbonate Depolymerization with a Cobalt Catalyst. *Inorg. Chem. Front.* **2024**. https://doi.org/10.1039/D3QI01833D.
(25) Kumar, A.; Von Wolff, N.; et al. Hydrogenative Depolymerization of Nylons. *J. Am. Chem. Soc.* **2020**, *142* (33), 14267–14275. https://doi.org/10.1021/jacs.0c05675.
(26) Zhou, W.; Neumann, P.; et al. Depolymerization of Technical-Grade Polyamide 66 and Polyurethane Materials through Hydrogenation. *ChemSusChem* **2021**, *14* (19), 4176–4180. https://doi.org/10.1002/cssc.202002465.
(27) Nallagangula, M.; Subaramanian, M.; et al. Transition Metal-Catalysis in Interrupted Borrowing Hydrogen Strategy. *Chem. Commun.* **2023**, *59* (51), 7847–7862. https://doi.org/10.1039/d3cc01517c.
(28) Kloxin, C. J.; Scott, T. F.; et al. Covalent Adaptable Networks (CANs): A Unique Paradigm in Cross-Linked Polymers. *Macromolecules* **2010**, *43* (6), 2643–2653. https://doi.org/10.1021/ma902596s.
(29) Montarnal, D.; Capelot, M.; et al. Silica-Like Malleable Materials from Permanent Organic Networks. *Science (80-.).* **2011**, *334* (6058), 965–968. https://doi.org/10.1126/science.1212648.
(30) Eck, M.; Schwab, S. T.; et al. Biodegradable High-Density Polyethylene-like Material. *Angew. Chem. Int. Ed.* **2023**, *62* (6), 1–4. https://doi.org/10.1002/anie.202213438.
(31) Häußler, M.; Eck, M.; et al. Closed-Loop Recycling of Polyethylene-like Materials. *Nature* **2021**, *590* (7846), 423–427. https://doi.org/10.1038/s41586-020-03149-9.
(32) Qian, X.; Han, D.; et al. High-Entropy Polymer Produces a Giant Electrocaloric Effect at Low Fields. *Nature* **2021**, *600* (7890), 664–669. https://doi.org/10.1038/s41586-021-04189-5.
(33) Yu, Z.; Zhou, H.; et al. Colossal Barocaloric Effect Achieved by Exploiting the Amorphous High Entropy of Solidified Polyethylene Glycol. *NPG Asia Mater.* **2022**, *14* (1). https://doi.org/10.1038/s41427-022-00448-7.
(34) *Functional Polymers by Post-Polymerization Modification*; Theato, P., Klok, H., Eds.; Wiley, 2012. https://doi.org/10.1002/9783527655427.
(35) Gauthier, M. A.; Gibson, M. I.; et al. Synthesis of Functional Polymers by Post-Polymerization Modification. *Angew. Chem. Int. Ed.* **2009**, *48* (1), 48–58. https://doi.org/10.1002/anie.200801951.
(36) Blasco, E.; Sims, M. B.; et al. 50th Anniversary Perspective: Polymer Functionalization. *Macromolecules* **2017**, *50* (14), 5215–5252. https://doi.org/10.1021/acs.macromol.7b00465.
(37) Zhukhovitskiy Maxim; Ditzler, Rachael A. J., A. V. . R. Advancing the Logic of Polymer Synthesis via Skeletal Rearrangements. *Synlett* **2022**, *33* (15), 1481–1485. https://doi.org/10.1055/s-0041-1737456.
(38) Hirai, T.; Yagi, K.; et al. High-Entropy Polymer Blends Utilizing in Situ Exchange Reaction. *Polymer (Guildf).* **2022**, *240* (October 2021), 124483. https://doi.org/10.1016/j.polymer.2021.124483.
(39) Huang, Y. J.; Yeh, J. W.; et al. "High-Entropy Polymers": A New Route of Polymer Mixing with Suppressed Phase Separation. *Materialia* **2021**, *15* (September 2020), 100978. https://doi.org/10.1016/j.mtla.2020.100978.
(40) Ditzler, R. A. J.; King, A. J.; et al. Editing of Polymer Backbones. *Nat. Rev. Chem.* **2023**, *7* (9), 600–615. https://doi.org/10.1038/s41570-023-00514-w.
(41) Takata, T.; Yamamoto, K.; et al. Efficient Transformation of Polymer Main Chain Catalyzed by Macrocycle Metal Complexes via Pseudorotaxane Intermediate. *Angew. Chem. Int. Ed.* **2023**, *62* (24). https://doi.org/10.1002/anie.202303494.
(42) Schäfer, M.; Yuan, S.; et al. Asymmetric Co-Unit Inclusion in Statistical Copolyesters. *Macromolecules* **2021**, *54* (2),

835–845. https://doi.org/10.1021/acs.macromol.0c01965.
(43) Dubey, A.; Khaskin, E. Catalytic Ester Metathesis Reaction and Its Application to Transfer Hydrogenation of Esters. *ACS Catal.* **2016**, *6* (6), 3998–4002. https://doi.org/10.1021/acscatal.6b00827.
(44) Tetsuka, H.; Doi, Y.; et al. Synthesis and Thermal Properties of Novel Periodic Poly(Ester - Amide)s Derived from Adipate, Butane-1,4-Diamine, and Linear Aliphatic Diols. *Macromolecules* **2006**, *39* (8), 2875–2885. https://doi.org/10.1021/ma052566j.
(45) *For Details, Please See the Supporting Information.*
(46) Alig, L.; Fritz, M.; et al. First-Row Transition Metal (De)Hydrogenation Catalysis Based on Functional Pincer Ligands. *Chem. Rev.* **2019**, *119* (4), 2681–2751. https://doi.org/10.1021/acs.chemrev.8b00555.
(47) Kallmeier, F.; Kempe, R. Manganese Complexes for (De)Hydrogenation Catalysis: A Comparison to Cobalt and Iron Catalysts. *Angew. Chem. Int. Ed.* **2018**, *57* (1), 46–60. https://doi.org/10.1002/anie.201709010.
(48) Kumar, A.; Janes, T.; et al. Manganese Catalyzed Hydrogenation of Organic Carbonates to Methanol and Alcohols. *Angew. Chem. Int. Ed.* **2018**, *57* (37), 12076–12080. https://doi.org/10.1002/anie.201806289.
(49) Schlagbauer, M.; Kallmeier, F.; et al. Manganese-Catalyzed B-Methylation of Alcohols by Methanol. *Angew. Chem.* **2020**, *132* (4), 1501–1506. https://doi.org/10.1002/ange.201912055.
(50) Bertini, F.; Glatz, M.; et al. Carbon Dioxide Hydrogenation Catalysed by Well-Defined Mn(i) PNP Pincer Hydride Complexes. *Chem. Sci.* **2017**, *8* (7), 5024–5029. https://doi.org/10.1039/c7sc00209b.
(51) Xia, T.; Spiegelberg, B.; et al. Manganese PNP-Pincer Catalyzed Isomerization of Allylic/Homo-Allylic Alcohols to Ketones-Activity, Selectivity, Efficiency. *Catal. Sci. Technol.* **2019**, *9* (22), 6327–6334. https://doi.org/10.1039/c9cy01502g.
(52) Tang, S.; Milstein, D. Template Catalysis by Manganese Pincer Complexes: Oxa- and Aza-Michael Additions to Unsaturated Nitriles. *Chem. Sci.* **2019**, *10* (39), 8990–8994. https://doi.org/10.1039/c9sc03269j.
(53) Espinosa-Jalapa, N. A.; Nerush, A.; et al. Manganese-Catalyzed Hydrogenation of Esters to Alcohols. *Chem. - A Eur. J.* **2017**, *23* (25), 5934–5938. https://doi.org/10.1002/chem.201604991.
(54) Das, U. K.; Janes, T.; et al. Manganese Catalyzed Selective Hydrogenation of Cyclic Imides to Diols and Amines. *Green Chem.* **2020**, *22* (10), 3079–3082. https://doi.org/10.1039/d0gc00570c.
(55) Freitag, F.; Irrgang, T.; et al. Mechanistic Studies of Hydride Transfer to Imines from a Highly Active and Chemoselective Manganate Catalyst. *J. Am. Chem. Soc.* **2019**, *141* (29), 11677–11685. https://doi.org/10.1021/jacs.9b05024.
(56) Gawali, S. S.; Pandia, B. K.; et al. Manganese(I)-Catalyzed Cross-Coupling of Ketones and Secondary Alcohols with Primary Alcohols. *ACS Omega* **2019**, *4* (6), 10741–10754. https://doi.org/10.1021/acsomega.9b01246.
(57) Glatz, M.; Stöger, B.; et al. Chemoselective Hydrogenation of Aldehydes under Mild, Base-Free Conditions: Manganese Outperforms Rhenium. *ACS Catal.* **2018**, *8* (5), 4009–4016. https://doi.org/10.1021/acscatal.8b00153.
(58) Gorgas, N.; Kirchner, K. Isoelectronic Manganese and Iron Hydrogenation/Dehydrogenation Catalysts: Similarities and Divergences. *Acc. Chem. Res.* **2018**, *51* (6), 1558–1569. https://doi.org/10.1021/acs.accounts.8b00149.
(59) Hert, C. M.; Curley, J. B.; et al. Comparative CO2Hydrogenation Catalysis with MACHO-Type Manganese Complexes. *Organometallics* **2022**, *41* (22), 3332–3340. https://doi.org/10.1021/acs.organomet.2c00295.
(60) Mukherjee, A.; Nerush, A.; et al. Manganese-Catalyzed Environmentally Benign Dehydrogenative Coupling of Alcohols and Amines to Form Aldimines and H2: A Catalytic and Mechanistic Study. *J. Am. Chem. Soc.* **2016**, *138* (13), 4298–4301. https://doi.org/10.1021/jacs.5b13519.
(61) Mukherjee, A.; Milstein, D. Homogeneous Catalysis by Cobalt and Manganese Pincer Complexes. *ACS Catal.* **2018**, *8* (12), 11435–11469. https://doi.org/10.1021/acscatal.8b02869.
(62) Owen, A. E.; Preiss, A.; et al. Manganese-Catalyzed Dehydrogenative Synthesis of Urea Derivatives and Polyureas. *ACS Catal.* **2022**, *12*, 6923–6933. https://doi.org/10.1021/acscatal.2c00850.
(63) Elangovan, S.; Topf, C.; et al. Selective Catalytic Hydrogenations of Nitriles, Ketones, and Aldehydes by Well-Defined Manganese Pincer Complexes. *J. Am. Chem. Soc.* **2016**, *138* (28), 8809–8814. https://doi.org/10.1021/jacs.6b03709.
(64) Andérez-Fernández, M.; Vogt, L. K.; et al. A Stable Manganese Pincer Catalyst for the Selective Dehydrogenation of Methanol. *Angew. Chem. Int. Ed.* **2017**, *56* (2), 559–562. https://doi.org/10.1002/anie.201610182.
(65) Duarte de Almeida, L.; Bourriquen, F.; et al. Catalytic Formal Hydroamination of Allylic Alcohols Using Manganese PNP-Pincer Complexes. *Adv. Synth. Catal.* **2021**, *363* (17), 4177–4181. https://doi.org/10.1002/adsc.202100081.
(66) Wei, D.; Sang, R.; et al. Reversible Hydrogenation of Carbon Dioxide to Formic Acid Using a Mn-Pincer Complex in the Presence of Lysine. *Nat. Energy* **2022**, *7* (5), 438–447. https://doi.org/10.1038/s41560-022-01019-4.
(67) Babu, R.; Padhy, S. S.; et al. Expedient Tandem Dehydrogenative Alkylation and Cyclization Reactions under Mn(i)-Catalysis. *Catal. Sci. Technol.* **2023**, *13* (9), 2763–2771. https://doi.org/10.1039/d3cy00009e.
(68) Sivakumar, G.; Subaramanian, M.; et al. Single-Molecular Mn(I)-Complex-Catalyzed Tandem Double Dehydrogenation Cross-Coupling of (Amino)Alcohols under Solventless Conditions with the Liberation of H2and H2O. *ACS Sustain. Chem. Eng.* **2022**, *10* (22), 7362–7373. https://doi.org/10.1021/acssuschemeng.2c01222.
(69) Yadav, V.; Landge, V. G.; et al. Manganese-Catalyzed α-Olefination of Nitriles with Secondary Alcohols. *ACS Catal.* **2020**, *10* (2), 947–954. https://doi.org/10.1021/acscatal.9b02811.
(70) Pérez-Camargo, R. A.; Fernández-d'Arlas, B.; et al. Tailoring the Structure, Morphology, and Crystallization of Isodimorphic Poly(Butylene Succinate- Ran -Butylene Adipate) Random Copolymers by Changing Composition and Thermal History. *Macromolecules* **2017**, *50* (2), 597–608. https://doi.org/10.1021/acs.macromol.6b02457.
(71) Pepels, M. P. F.; Govaert, L. E.; et al. Influence of the Main-Chain Configuration on the Mechanical Properties of Linear Aliphatic Polyesters. *Macromolecules* **2015**, *48* (16), 5845–5854. https://doi.org/10.1021/acs.macromol.5b01089.
(72) Bittiger, H.; Marchessault, R. H.; et al. Crystal Structure of Poly-ε-Caprolactone. *Acta Crystallogr. Sect. B Struct. Crystallogr. Cryst. Chem.* **1970**, *26* (12), 1923–1927. https://doi.org/10.1107/S0567740870005198.
(73) Gestí, S.; Almontassir, A.; et al. Crystalline Structure of Poly(Hexamethylene Adipate). Study on the Morphology and the Enzymatic Degradation of Single Crystals. *Biomacromolecules* **2006**, *7* (3), 799–808. https://doi.org/10.1021/bm050860d.
(74) Rohindra, D.; Lata, R.; et al. Crystallization Behavior in Miscible Blends of Poly(E-caprolactone) and Poly(Hexylene Adipate) with Similar Thermal Properties Studied by Time-resolved Fourier Transform Infrared Spectroscopy. *Polym. Cryst.* **2019**, *2* (1). https://doi.org/10.1002/pcr2.10037.
(75) Li, X.; Hong, Z.; et al. Identifying the Phase Behavior of Biodegradable Poly(Hexamethylene Succinate-Co-Hexamethylene Adipate) Copolymers with FTIR. *J. Phys. Chem. B* **2009**, *113* (9), 2695–2704. https://doi.org/10.1021/jp8061866.

(76) Stanton, M. G. “New” Catalysts for the Ester-Interchange Reaction: The Role of Alkali-Metal Alkoxide Clusters in Achieving Unprecedented Reaction Rates. *J. Am. Chem. Soc.* **1998**, *120* (24), 5981–5989. https://doi.org/10.1021/ja980584t.
(77) Spasyuk, D.; Smith, S.; et al. Replacing Phosphorus with Sulfur for the Efficient Hydrogenation of Esters. *Angew. Chem. Int. Ed.* **2013**, *52* (9), 2538–2542. https://doi.org/10.1002/anie.201209218.
(78) Rummel, F.; Wehmeyer, F.; et al. Slow Inversion of Coordinated Thioether Groups in SNS-Type Ruthenium Pincer Complexes. *Eur. J. Inorg. Chem.* **2023**, *26* (28). https://doi.org/10.1002/ejic.202300313.
(79) Dub, P. A.; Gordon, J. C. Metal-Ligand Bifunctional Catalysis: The “Accepted” Mechanism, the Issue of Concertedness, and the Function of the Ligand in Catalytic Cycles Involving Hydrogen Atoms. *ACS Catal.* **2017**, *7* (10), 6635–6655. https://doi.org/10.1021/acscatal.7b01791.
(80) Rauch, M.; Luo, J.; et al. Mechanistic Investigations of Ruthenium Catalyzed Dehydrogenative Thioester Synthesis and Thioester Hydrogenation. *ACS Catal.* **2021**, *11* (5), 2795–2807. https://doi.org/10.1021/acscatal.1c00418.
(81) Hou, C.; Jiang, J.; et al. When Bifunctional Catalyst Encounters Dual MLC Modes: DFT Study on the Mechanistic Preference in Ru-PNNH Pincer Complex Catalyzed Dehydrogenative Coupling Reaction. *ACS Catal.* **2017**, *7* (1), 786–795. https://doi.org/10.1021/acscatal.6b02505.
(82) Alberico, E.; Lennox, A. J. J.; et al. Unravelling the Mechanism of Basic Aqueous Methanol Dehydrogenation Catalyzed by Ru-PNP Pincer Complexes. *J. Am. Chem. Soc.* **2016**, *138* (45), 14890–14904. https://doi.org/10.1021/jacs.6b05692.
(83) Gusev, D. G. Dehydrogenative Coupling of Ethanol and Ester Hydrogenation Catalyzed by Pincer-Type YNP Complexes. *ACS Catal.* **2016**, *6* (10), 6967–6981. https://doi.org/10.1021/acscatal.6b02324.
(84) Armarego, W. L. F. *Purification of Laboratory Chemicals*; Elsevier: Oxford.
(85) Dolomanov, O. V.; Bourhis, L. J.; et al. OLEX2 : A Complete Structure Solution, Refinement and Analysis Program. *J. Appl. Crystallogr.* **2009**, *42* (2), 339–341. https://doi.org/10.1107/S0021889808042726.
(86) Bourhis, L. J.; Dolomanov, O. V.; et al. The Anatomy of a Comprehensive Constrained, Restrained Refinement Program for the Modern Computing Environment - Olex2 Dissected. *Acta Crystallogr. Sect. A Found. Crystallogr.* **2015**, *71* (1), 59–75. https://doi.org/10.1107/S2053273314022207.
(87) Sheldrick, G. M. A Short History of SHELX. *Acta Crystallogr. Sect. A Found. Crystallogr.* **2008**, *64* (1), 112–122. https://doi.org/10.1107/S0108767307043930.
(88) Sheldrick, G. M. SHELXT - Integrated Space-Group and Crystal-Structure Determination. *Acta Crystallogr. Sect. A Found. Crystallogr.* **2015**, *71* (1), 3–8. https://doi.org/10.1107/S2053273314026370.
(89) Torchia, D. A. Volume 30, No. 3 (1978), to the Communication, “The Measurement of Proton-Enhanced Carbon-13 T1 Values by a Method Which Suppresses Artifacts.” *J. Magn. Reson.* **1979**, *33* (2), 481. https://doi.org/10.1016/0022-2364(79)90267-1.
(90) Derbyshire, W.; van den Bosch, M.; et al. Fitting of the Beat Pattern Observed in NMR Free-Induction Decay Signals of Concentrated Carbohydrate–Water Solutions. *J. Magn. Reson.* **2004**, *168* (2), 278–283. https://doi.org/10.1016/j.jmr.2004.03.013.
(91) Hohenberg, P.; Kohn, W. Inhomogeneous Electron Gas. *Phys. Rev.* **1964**, *136* (3B), B864–B871. https://doi.org/10.1103/PhysRev.136.B864.
(92) Frisch, M. J.; Trucks, G. W.; et al. Gaussian 16. Gaussian, Inc.: Wallingford CT 2016.
(93) Weigend, F.; Hättig, C.; et al. Accurate Coulomb-Fitting Basis Sets for H to Rn. *Phys. Chem. Chem. Phys.* **2006**, *8* (9), 1057. https://doi.org/10.1039/b515623h.
(94) Weigend, F.; Ahlrichs, R.; et al. Balanced Basis Sets of Split Valence, Triple Zeta Valence and Quadruple Zeta Valence Quality for H to Rn: Design and Assessment of Accuracy. *Phys. Chem. Chem. Phys.* **2005**, *7* (18), 3297. https://doi.org/10.1039/b508541a.
(95) Marenich, A. V.; Cramer, C. J.; et al. Universal Solvation Model Based on Solute Electron Density and on a Continuum Model of the Solvent Defined by the Bulk Dielectric Constant and Atomic Surface Tensions. *J. Phys. Chem. B* **2009**, *113* (18), 6378–6396. https://doi.org/10.1021/JP810292N/SUPPL_FILE/JP810292N_SI_003.PDF.